Aircraft Evaluation of MODIS Cloud Drop Number Concentration Retrievals

Scarlet R. Passer[1], Mikael K. Witte[2], and Patrick Y. Chuang[1]

[1]Earth and Planetary Sciences, University of California Santa Cruz, Santa Cruz, CA, USA
[2]Department of Meteorology, Naval Postgraduate School, Monterey, CA, USA

Correspondence: Patrick Y. Chuang (pchuang@ucsc.edu)

Abstract. Cloud ~~droplet~~ drop number concentration (~~N_d~~ N_d) can be retrieved through passive satellite observation. These retrievals are useful due to their wide spatial and temporal coverage. However, the accuracy of the retrieved values is not well understood. In this ~~paper, we compare satellite N_d~~ study, we seek to understand why the retrievals agree or disagree with in situ measurements by examining the various cloud properties that underlie the retrievals. To do so, we compare satellite N_d derived from the Moderate Resolution Imaging Spectroradiometer (MODIS) instrument with in situ aircraft measurements using a phase Doppler interferometer onboard three flight campaigns sampling marine stratocumulus clouds. Intercomparison of ~~N_d~~ N_d values shows that the discrepancy between retrieved and in situ ~~N_d~~ N_d can be $\pm 50\%$ or more. In the mean, there is evidence of an overestimation bias by MODIS retrievals, although the sample size is insufficient for statistical certainty. We find that MODIS ~~N_d~~ N_d is best interpreted as representative of the mid-cloud region, as there is almost always a greater discrepancy from in situ values near cloud top and cloud base. We also find evidence of cases where ~~N_d~~ N_d is accurately retrieved, but effective radius is not, presumably due to offsetting errors in other retrieval parameters. Vertical profiles of extinction coefficient β, liquid water content L, and effective radius ~~r_e~~ r_e measured during sawtooth-pattern flight legs through cloud top are also compared to implicit MODIS retrieval profiles. For the ~~one case with N_d~~ two cases with N_d agreement, all profiles match well. For ~~seven~~ the six cases with significant disagreement, there is no consistent underlying cause. The discrepancy originates from either: (a) discrepancy in the ~~r_e~~ r_e profile, (b) discrepancy in the β and L profiles, or (c) discrepancy in both.

1 Introduction

Cloud drop number concentration (~~N_d~~ N_d) is a fundamental property of clouds. This ~~quantity~~ property is relevant to ~~cloud properties that impact~~ numerous effects that clouds have on weather and climate~~, such as cloud radiative effects, precipitation, and~~ . For example, clouds with higher N_d will have a larger albedo (assuming all else equal), which in turn will lead to a larger solar reflectance (Twomey, 1977). The ability of a warm (i.e., ice-free) cloud to form precipitation is also dependent on N_d. A cloud with very high N_d will not produce appreciable rainfall rates since the drops are unable to grow to the required sizes to efficiently sediment, while at the other extreme of very low N_d, warm clouds produce precipitation very effectively (Sorooshian et al., 2009). Understanding and evaluating aerosol-cloud interactions ~~.~~ frequently involves N_d, since activation of

particulate matter is one of the strongest connections between aerosol and clouds (Bellouin et al., 2020; Quaas et al., 2020; Gordon et al., 20
.

Passive satellite observation is one of the primary methods that we have to measure and understand the climatology of N_d N_d at large spatial and temporal scales (e.g., Bennartz, 2007; McCoy et al., 2018, 2020; Christensen et al., 2022). The Moderate Resolution Imaging Spectroradiometer (MODIS) instrument onboard the Terra and Aqua satellites is one important source of such observations . However, the estimation of N_d relies on assumptions which may or may not portray cloud properties accurately in all situations. satellite observations of N_d. A review paper by Grosvenor et al. (2018) comprehensively surveys our understanding of N_d derived from remote sensing, so we focus this Introduction only on aspects that are directly relevant for this study. A theoretical analysis by Bennartz (2007) suggests that for cloud fractions over 80% and LWP>30 g/m^2, i.e., conditions relevant to the stratocumulus (Sc) clouds observed in this study, MODIS N_d retrievals should exhibit relative errors < 80%, a value which Grosvenor et al. (2018) is in agreement with. These errors are mainly due to uncertainties in retrieving r_e, LWP, cloud optical depth τ_c, and cloud fraction.

There are a handful of past studies that assess the agreement between in situ aircraft measurements and satellite retrievals of N_d. Painemal and Zuidema (2011) use data from the National Center for Atmospheric Research (NCAR) C-130 aircraft measuring Sc in the SE Pacific during VOCALS. They find good agreement in the mean for the 19 cases that they examined, while using the assumption that the liquid water profile is adiabatic. Two of the 19 cases had large discrepancies (30 to 50% discrepancy) that they attribute to sub-adiabaticity. Their cases span a wide range, from <50 cm^{-3} to >300 cm^{-3}. They also find that the assumption that N_d is constant with height was valid for their cases. However, Grosvenor et al. (2018) point out that their strong agreement is not necessarily because the underlying measurements are accurate, but due to an overestimate of the effective radius almost exactly offsetting an overestimate of the cloud adiabaticity. Min et al. (2012) also analyze data from VOCALS, but combine NCAR C-130 and US Department of Energy (DOE) G-1 aircraft data, and find that, without accounting for adiabaticity, MODIS overestimates N_d relative to aircraft measurements, with a mean bias of 25%. If measured adiabaticity is used, then no statistically significant bias is detected, with most of their 17 cases appearing to agree to within 50% (two outliers are noted). A third study (Bennartz and Rausch, 2017) compared results from their updated algorithm to the same VOCALS results as Painemal and Zuidema (2011). They find a modest bias (less than 20 cm^{-3}) between aircraft and MODIS, and an average uncertainty of $\sim$ 35 cm^{-3}. McCoy et al. (2018) utilize a much larger data set, but in order to do so, they greatly relaxed the requirements for co-location of aircraft and satellite observations in both space and time. They compare aircraft measurements with the satellite retrieval averaged over 3 days for the closest 3°× 3° area. They find average agreement to be much poorer than these previous studies (r^2=0.46), but this may simply be a matter of not measuring the same cloud at the same time.

Gryspeerdt et al. (2022) compared many aircraft field campaigns with satellite retrieved N_d, although only a subset of these are focused on stratiform clouds. Their data set is a mixture of different instruments and different aircraft platforms. If we examine their results only from Sc projects, they find r^2 values between 0.5 and 0.75. Restricting the data using different filters can somewhat increase r^2, though the range for Sc-only campaigns remains about the same. The best-fit slope of the in situ vs. MODIS data for Sc-only campaigns is, with one exception (discussed next), close to 1, suggesting no mean bias.

Variability of the data is high, however, with many measurements disagreeing by a factor of 2 or more. The one project that is the exception, i.e. exhibits significant bias between in situ and satellite derived N_d is, surprisingly, from the analysis of NCAR C-130 data from VOCALS. The slope is very noticeably different from 1, with MODIS exhibiting larger values relative to aircraft. This result appears to disagree with the three other studies that focus on VOCALS (described above). The source of this disagreement is unclear.

Broadly speaking, these comparisons, with some exceptions, paint a rather optimistic picture for N_d retrievals. Most of these studies suggest that MODIS retrievals are better than the theoretical 80% relative uncertainty proposed by Bennartz (2007), albeit these are not all the same retrievals (many of the studies filter the data in various ways to assess which conditions are most favorable for an accurate retrieval). However, given that many of these studies focus on the VOCALS field campaign and utilize in situ cloud probes with the same operating principle (with Gryspeerdt et al., 2022, being the exception to both) , it would be informative to broaden the type of cloud and instrument used for evaluating satellite N_d retrievals. There are reasons to believe that the in situ measurements onboard the C-130 from the VOCALS campaign may have biases. Past studies (e.g. Painemal and Zuidema, 2011) attribute biases between in situ and MODIS-retrieved effective radius during VOCALS to issues with the satellite retrievals (e.g., due to three-dimensional radiative effects or unresolved horizontal heterogeneity). However, Witte et al. (2018), using aircraft data from a phase Doppler interferometer (PDI) during three different Sc field campaigns, found no bias between in situ and MODIS r_e. They find that the bias when using the older cloud probes is correlated with the breadth of the drop size distribution, which they attribute to difficulties that such probes have measuring larger drops. However, this issue may affect estimation of r_e differently than for N_d, so it is unclear what the consequences are, if any, of such instrument limitations.

The focus of this study is to understand and compare MODIS retrievals against in situ measurements from three Sc-focused field campaigns using PDI data from the Twin Otter in order to evaluate the accuracy of the satellite N_d product. In addition, we seek to identify the underlying cause of any discrepancies observed between MODIS and in situ observationsN_d product. These are the same data sets as used in Witte et al. (2018). Importantly, we will also evaluate the validity of the assumptions underlying the retrievals through analysis of vertical profiles of cloud properties, which, to our knowledge, previous studies have not examined in detail. When we find good agreement, is it because the underlying properties are also in agreement, or are there cases of compensating canceling errors? When we find poor agreement, is there one consistent reason for it, or is there a diversity of reasons? A review paper by Grosvenor et al. (2018) comprehensively surveys our understanding of deriving N_d from remote sensing, so we focus this Introduction only on aspects that are directly relevant for this study.

1.1 MODIS N_d Retrieval Satellite N_d retrieval

The most common MODIS retrieval of number concentration utilizes the following equation (Grosvenor et al., 2018):

$$N_{d\mathrm{d}} = \frac{\sqrt{5}}{2\pi k}\left(\frac{f_{ad}c_w\tau_c}{Q_{ext}\rho_w r_e^5}\frac{f_\mathrm{ad}c_\mathrm{w}\tau_\mathrm{c}}{Q_\mathrm{ext}\rho_\mathrm{w} r_\mathrm{e}^5}\right)^{1/2} \qquad (1)$$

Cloud optical depth ~~τ_c~~ τ_{c} and cloud top effective radius ~~r_e~~ r_{e} are the two (mostly) independently retrieved quantities ~~in the MODIS N_d retrieval . Retrieved N_d~~ used in the N_{d} retrieval where r_{e} is defined as:

$$r_e = \frac{\int_0^\infty r^3 n(r) dr}{\int_0^\infty r^2 n(r) dr} \tag{2}$$

where $n(r)$ is the drop size distribution as a function of drop radius r. Retrieved N_{d} is more sensitive to the same relative uncertainty in retrieved ~~r_e than τ_c~~ r_{e} than τ_{c} due to the difference in the magnitude of the exponents (5/2 versus 1/2) in Eq. 1. Density of water ~~ρ_w~~ ρ_{w} is known, and the remaining variables (adiabatic fraction f_{ad}, water content lapse rate c_{w}, a constant that relates the mean-volume and effective radii k, and the extinction efficiency factor Q_{ext}) are considered fixed as described below. ~~In order to estimate r_e, MODIS makes use of~~ To produce an estimate of r_{e} from aircraft suitable for comparison with that from MODIS, a weighting function ~~, defined as (Platnick, 2000):~~ is used to weight the impact of cloud vertical structure on the aircraft-derived variables (Platnick, 2000):

$$W(\tau_{\underline{c}\mathrm{c}}) = a\tau_{\mathrm{c}}{}^b exp\underline{(}\left(-\tau_{\underline{c}(}{}_{\mathrm{c}}\left(\frac{1}{\mu}+\frac{1}{\mu_0}\underline{))}\right)\right) \tag{3}$$

Here, $b = 2$, a is a normalization constant, and μ and μ_0 ~~depend on satellite position and correspond to the solar zenith angle and sensor zenith angle~~ are the cosine of the sensor and solar zenith angles, respectively. The weighting function describes, as a function of cloud optical depth, how much influence the measurement from a given region of a cloud has on satellite-derived variables. This function peaks within a few tens of meters of cloud top (Platnick, 2000; Witte et al., 2018), and therefore the effective radius reflects values in this cloud top region.

Cloud optical depth ~~τ_c~~ τ_{c} is defined as the vertical integral of the extinction coefficient $\beta(z)$:

$$\tau_{\underline{c}\mathrm{c}} = \int_{\underline{z_{base}}\, z_{\mathrm{base}}}^{\underline{z_{top}}\, z_{\mathrm{top}}} \beta(z) dz \tag{4}$$

where ~~z_{top} and z_{base}~~ z_{top} and z_{base} are the altitude of cloud top and cloud base, respectively.

At any altitude, $\beta(z)$ is related to the cloud drop size distribution ~~$n(r)$~~ $n(r,z)$, for which we now include the dependence on altitude z:

$$\beta(z) = \int_0^\infty \pi Q_{\underline{ext(r)}\,\mathrm{ext}} n(r,z) r^2 dr \tag{5}$$

The remaining variables in the ~~N_d~~ N_{d} retrieval (Eq. 1) are described as follows:

1. ~~N_d~~ N_{d} is assumed to be a constant with respect to height in the cloud, i.e. ~~$N_d(z) = constant$~~ $N_{\mathrm{d}}(z) = \mathrm{constant}$.

2. k is defined as:

$$k = \left(\frac{r_v}{r_e} \frac{r_\mathrm{v}}{r_\mathrm{e}} \right)^3 \tag{6}$$

where r_v r_v is volume-mean droplet drop radius. The MODIS retrieval assumes that $k = 0.8$. Previous studies suggest that k is well-constrained in stratocumulus clouds, typically ranging between 0.7 and 0.9 (Miles et al., 2000; Lebsock and Witte, 2023).

3. Q_{ext} Q_ext is the extinction efficiency (dimensionless), and represents the ratio between the extinction and physical geometric cross sections of a droplet. Because drop. It is a function of drop radius r, but because the radius of the droplets drops of interest is usually much larger than the wavelengths of light used for retrievals, MODIS assumes $Q_{ext} = 2$ the retrievals, it can be assumed $Q_\mathrm{ext} = 2$ (the limit for geometric optics) (Platnick, 2000).

4. c_w c_w is the adiabatic gradient of liquid water content L with respect to height, and is a weak function of temperature and pressure. From Eq. 14 in Grosvenor et al. (2018), we compute a value of $c_w = 2.3 \times 10^{-6}$ $c_\mathrm{w} = 2.3 \times 10^{-6}$ kg/m^4. We assume c_w c_w to be constant vertically through a cloud, which should introduce an error that is less than 1% since the stratocumulus observed in this study are quite geometrically thin (< 500 m) (Grosvenor et al., 2018).

5. f_{ad} f_ad is defined as the fraction of cloud liquid water content relative to its adiabatic value at a given height above cloud base. The MODIS retrieval assumes $f_{ad} = 0.6$. Combining the definitions of c_w and f_{ad} c_w and f_ad yields the profile of liquid water content:

$$L(z) = f_{ad\,\mathrm{ad}} c_{w\,\mathrm{w}} (z - z_{base\,\mathrm{base}}) \tag{7}$$

1.1.1 Retrieval Implicit retrieval profiles

The MODIS retrieval implicitly assumes specific vertical profiles of r_e r_e, β, and L. These profiles, along with cloud base height, can be derived starting with measured r_e and inferred N_d as follows:

1. The cloud top liquid water content is computed as:

$$L(z_{top\,\mathrm{top}}) = \frac{4}{3} \pi \rho_{w\,\mathrm{w}} \cdot k r_{e\,\mathrm{e}}^3 (z_\mathrm{top}) \cdot N_{d\,\mathrm{d}} \tag{8}$$

2. The liquid water content profile $L(z)$ is defined above (Eq. 7).

3. Cloud base height ~~z_{base}~~ z_{base} is determined by the altitude where $L(z) = 0$. By re-arranging Eq. 7 and applying it at ~~$z = z_{top}$~~ $z = z_{\mathrm{top}}$, we get:

$$z_{base\,\mathrm{base}} = z_{top\,\mathrm{top}} - L(z_{top\,\mathrm{top}})/f_{ad\,\mathrm{ad}}c_{w\,\mathrm{w}} \tag{9}$$

4. ~~$r_e(z)$~~ $r_{\mathrm{e}}(z)$ is derived starting from the definition of ~~r_v:~~ r_{v}:

$$\frac{4}{3}\pi r_{v\,\mathrm{v}}{}^3(z) N_{d\,\mathrm{d}} \rho_{w\,\mathrm{w}} = \frac{4}{3}\pi \left[k r_{e\,\mathrm{e}}{}^3(z) \right] N_{d\,\mathrm{d}} \rho_{w\,\mathrm{w}} = L(z)$$

which can be re-arranged in terms of ~~r_e:~~ r_{e}:

$$r_{e\,\mathrm{e}}(z) = \left[\frac{3}{4\pi\rho_w k} \frac{L(z)}{N_d} \frac{3}{4\pi\rho_{\mathrm{w}} k} \frac{L(z)}{N_{\mathrm{d}}} \right]^{1/3} \tag{10}$$

5. $\beta(z)$ is derived by substituting the definitions of ~~r_e~~ r_{e} and L into Eq. 5, which yields (Grosvenor et al., 2018):

$$\beta(z) = \frac{3}{4} \frac{Q_{ext}}{\rho_w} \frac{L(z)}{r_e(z)} \frac{Q_{\mathrm{ext}}}{\rho_{\mathrm{w}}} \frac{L(z)}{r_{\mathrm{e}}(z)} \tag{11}$$

In order to better identify the source of any discrepancies between MODIS and in situ ~~N_d, cloud base height z_{base}, along with~~ N_{d}, the vertical profiles ~~$r_e(z)$~~ $r_{\mathrm{e}}(z)$, $\beta(z)$, and $L(z)$ that are inherent in the MODIS algorithm for estimating ~~N_d~~ N_{d} will be compared to in situ observations of the same quantities, along with cloud base height z_{base}. There are a number of potential sources of uncertainty, including the MODIS retrievals of ~~r_e and τ_c~~ r_{e} and τ_{c}, as well as the validity of the above assumptions. ~~Grosvenor et al. (2018) estimates the overall uncertainty in retrieved N_d to be $\pm 25\%$.~~

2 Methods

2.1 In Situ Observations of ~~N_d~~ N_{d}

2.1.1 Aircraft Observations

In situ data was acquired during three different flight campaigns that sampled marine stratocumulus: the Marine Stratus/Stratocumulus Experiment (MASE; Lu et al., 2007), the Physics of Stratocumulus Top experiment (POST; Carman et al., 2012; Gerber et al., 2013), and the Variability of American Monsoon Systems Ocean-Cloud-Atmosphere-Land Study (VOCALS; Mechoso et al., 2014; Zheng et al., 2011). ~~Each campaign was flown on~~ All three of these campaigns used a phase Doppler interferometer (PDI) onboard the CIRPAS Twin Otter (TO) aircraft ~~with the same phase Doppler interferometer (PDI) that we~~

use to derive cloud microphysical properties. See Chuang et al. (2008) for details about the PDI measurement method and data processing.

The MASE campaign was flown in the NE Pacific near Monterey, California during July 2005. VOCALS was centered off the coast of Chile in the SE Pacific and was flown during October to November of 2008. The flight pattern of both Flights during the MASE and VOCALS campaigns was over level legs utilized level legs (i.e., flight segments flown at constant altitude and heading for a sustained period, usually 10 min for the flights analyzed in this work) which sampled from below cloud base to near cloud top. POST was flown slightly farther offshore in a similar location as MASE, during July and August of 2008. Flight legs used from From the POST campaign we analyze flight legs that were flown in a sawtooth pattern, flying repeatedly up and down between ~ 100 m below cloud top to ~ 100 m above. Overall, we analyze four flight days from MASE, ten from VOCALS, and eight from the POST campaign, as these flights coincide with a MODIS overpass. More details on matching the aircraft flights with MODIS overpasses can be found in Witte et al. (2018).

The PDI measurements from these three field campaigns have been used to analyze the retrieval of cloud effective radius from MODIS. Previous studies (Painemal and Zuidema, 2011; Min et al., 2012; Noble and Hudson, 2015) have suggested that MODIS retrievals of r_e r_{e} are biased high by 2 to 5 µm relative to in situ measurements, but using the same data set as in this study, Witte et al. (2018) found no such bias, with a discrepancy between MODIS and in situ mesurements that agrees, in the mean, to measurements agreeing within 0.7 µm . The bias is instead attributed in the mean. They attribute observed bias to issues with the in situ aircraft instrumentation used in previous studies. This suggests that, in the mean, there is no bias in retrievals of N_d N_{d} due to a bias in retrieved r_e r_{e}, an assertion that we will evaluate as part of our analysisin this study.

2.1.2 In Situ N_d N_{d} and r_e r_{e} Calculations

To estimate cloud drop number concentration from PDI, in-cloud sampling legs are chosen analyzed for each flightanalyzed. To be consistent with MODIS, cloud top data is data from near cloud top are used to derive r_e r_{e}. In contrast, because the satellite retrieval assumes N_d N_{d} is constant throughout the cloud, mid-cloud data is are used to derive number concentration, as this location is the most more representative of the cloud as a whole mean cloud N_{d} value relative to cloud top values (as will be discussed further shown below). Cloud top number concentration can be lower than mid-cloud values due to entrainment.

For the VOCALS and MASE campaigns, we analyze mid-cloud and cloud top legs are selected during flight by the flight scientistlevel legs. However, the POST campaign primarily used a sawtooth flight pattern. Therefore, we define cloud top as the altitude where liquid water content crosses a threshold of $L = 0.05$ g/m^3, a commonly used threshold in the airborne science community. Effective radius is calculated from within 10 m of this cloud top. Mid-cloud is defined by altitudes We use the range between 60 m to 90 m below cloud top and used to calculate number concentration. as an analog to level mid-cloud legs to calculate a representative value of N_{d} during POST. While this altitude range does not correspond to "mid-cloud" in the sense of cloud geometric thickness, this region is typically far enough from cloud top to avoid the impacts of entrainment mixing.

For ease in comparing MODIS implicit cloud profile estimations to observation, we create a shifted altitude ($z_{shift}$$z_{\mathrm{shift}}$) for POST which is defined by $z_{shift} = 0$ $z_{\mathrm{shift}} = 0$ at cloud top, i.e. $z_{shift} = z - z_{top}$$z_{\mathrm{shift}} = z - z_{\mathrm{top}}$. To perform this coordinate transformation, we determine the altitude of cloud top (~~z_{top}~~z_{top}) for each individual ascent or descent (or "leg") of the sawtooth flight path (using the threshold $L = 0.05$ g/m^3). All in situ measurements for each leg are referenced to ~~z_{shift}~~ z_{shift} for that leg. More details about the altitude shifting process can be found in Carman et al. (2012).

For the purpose of making a more like-to-like comparison between PDI and MODIS, number concentration and effective radius measured along their respective legs are averaged over 1 km (20 ~~sec) intervals , matching the~~ s) intervals to match MODIS spatial resolution. The mean and variability of ~~N_d and r_e for each flight~~ N_{d} and r_{e} for each 10 min (or ≈30 km at a mean true airspeed of 55 m/s) flight leg are calculated from these 1 km average values~~.~~, which is the uncertainty that we show in the results (below). This variability does not reflect any uncertainty due to differences in the spatial domain sampled, as well as any temporal differences in the sampling, which are difficult to assess.

The main source of instrumental uncertainty is the uncertainty in the instrument view volume. The view volume, in units of volume of air sampled per second, is the product of three values. The first is the probe "length", which is calculated for each flight from the collected data itself (using the method from Chuang et al., 2008), so day-to-day variation should be accounted to well within 5%. The second value is the aircraft true air speed, which is known quite accurately, almost certainly to within 5%. The third value is the probe "width", which is fixed by the optical hardware. Recent in-depth laboratory examination of this subject (Leandro, 2023) suggests that this width may be smaller than the theoretical value for very small drops, which would lead to an under-estimation of N_{d}, but mostly affect larger values of N_{d} (which tend to exhibit smaller drop sizes). We estimate that this bias could be as large as 10% for $N_{\text{d}} > 400$ cm^{-3} and decreases to less than 1% for $N_{\text{d}} < 100$ cm^{-3}. Counting uncertainty is unlikely to be significant because many thousands of drops are observed for any given data point, so the Poisson standard deviation of $\sqrt{n}$ would suggest an uncertainty of < 1%. These instrumental uncertainties, when combined, produce an uncertainty of less than 20%, which is almost always smaller than the observed spatiotemporal variability, which is why we report the latter.

2.1.3 Profile Calculations

~~To estimate N_d, MODIS~~ The N_{d} retrieval combines measurements of ~~τ_c~~ τ_{c} and cloud top ~~r_e~~ r_{e} with assumptions about the cloud vertical structure (see Section 1.1). Therefore, ~~MODIS implicitly assumes~~ specific vertical profiles of effective radius, liquid water content, and extinction coefficient are implicitly assumed. Due to the sawtooth sampling strategy during the POST campaign, we can compare these assumed profiles with observations. We also evaluate the assumptions that k and ~~f_{ad}~~ f_{ad} are constant.

Profiles of L, ~~r_e~~r_{e}, and β are derived directly from cloud drop size ~~distribution~~ distributions measured by the PDI and binned over 5 m increments within ~~z_{shift}~~ z_{shift} space. Consistent with the ~~MODIS scheme~~satellite retrieval (Eq. 1), we also assume ~~$Q_{ext} = 2$~~ $Q_{\text{ext}} = 2$ when calculating β. To determine ~~$L_{ad}(z)$~~the adiabatic liquid water content $L_{\text{ad}}(z)$, first the mean altitude for near-cloud base is identified using a threshold liquid water content of $L = 0.1$ g/m^3. Next, ~~c_w~~ c_{w} is used to extrapolate downward to $L = 0$ g/m^3 associated with the true cloud base ~~z_{base}~~z_{base}.

2.2 Satellite retrieval details and sampling methodology

~~In order to determine MODIS number concentration, 1 km retrievalsof r_e and τ_c are taken from satellite swaths that match both the temporal and spatial location of the PDI flight campaigns (for more details on temporal matching, see Witte et al., 2018)~~ We utilize MODIS collection 6.1 level 2 retrievals of r_e and τ_c using the 2.1 μm band ("Cloud_Effective_Radius" and "Cloud_Optical_Thickness" products, respectively) from both Aqua and Terra, consistent with the approach of Witte et al. (2018) . Over the small sample size considered here, we find no evidence of systematic differences between satellites. Number concentration N_d is then calculated from r_e and τ_c using Eq. 1. A full description of the MODIS sampling methodology is given in Witte et al. (2018). Briefly, we analyze flight legs that occurred within 90 min of MODIS overpasses that covered the flight sampling area (most retrievals were within 30 min of their associated aircraft leg). We then ~~average these measurements over~~ select a 25 km^2 (5×5 pixels) ~~in order~~ area centered on the mean coordinates of the aircraft leg to compare with in situ measurements. ~~MODIS N_d is then estimated using Eq. 1 as described in Section 1.1.~~

2.3 Uncertainty calculations

Uncertainty of any variable x is expressed as the ~~standard error:~~ 95% margin of error:

$$error = \frac{\sigma_x}{\sqrt{n_x}} * z z(0.95) \tag{12}$$

where σ_x is the standard deviation of x, ~~and~~ n_x represents the total number of measurements~~. The~~ , and the quantity $z(0.95)$ is the z-score for the 95% confidence interval and has a value of 1.96. We choose margin of error versus standard error to reflect uncertainty in unsampled spatial variability since the aircraft samples a narrow transect through a 1×1 km^2 box while MODIS senses photons arriving from the entire area.

The MODIS uncertainty is calculated from 1 km measurements over a 25 km^2 area. PDI uncertainty is calculated from downsampled 1 km measurements over the relevant time interval of a given flight leg. Both the MODIS and PDI uncertainties are a reflection of spatial variability at 1 km. This measurement does not reflect instrumental uncertainty or error in assumptions.

3 Results

We first analyze ~~N_d~~ N_d and ~~r_e~~ r_e for all three campaigns. After that, we capitalize on the sawtooth legs from the POST flights to compare profiles of k, ~~f_{ad}, r_e~~ f_ad, r_e, β, and L.

3.1 Comparison between MODIS and PDI ~~N_d~~ N_d

Fig. 1 compares MODIS and PDI ~~N_d~~ N_d for all three flight campaigns. Though the majority of flights agree to within ~~25~~50% (accounting for variability), there are several cases that exceed this range. Of those cases, most are overestimates by MODIS, with the one exception being VOCALS day 2008/11/01 (teal diamond in Fig. 1). At a population level, linear regression yields

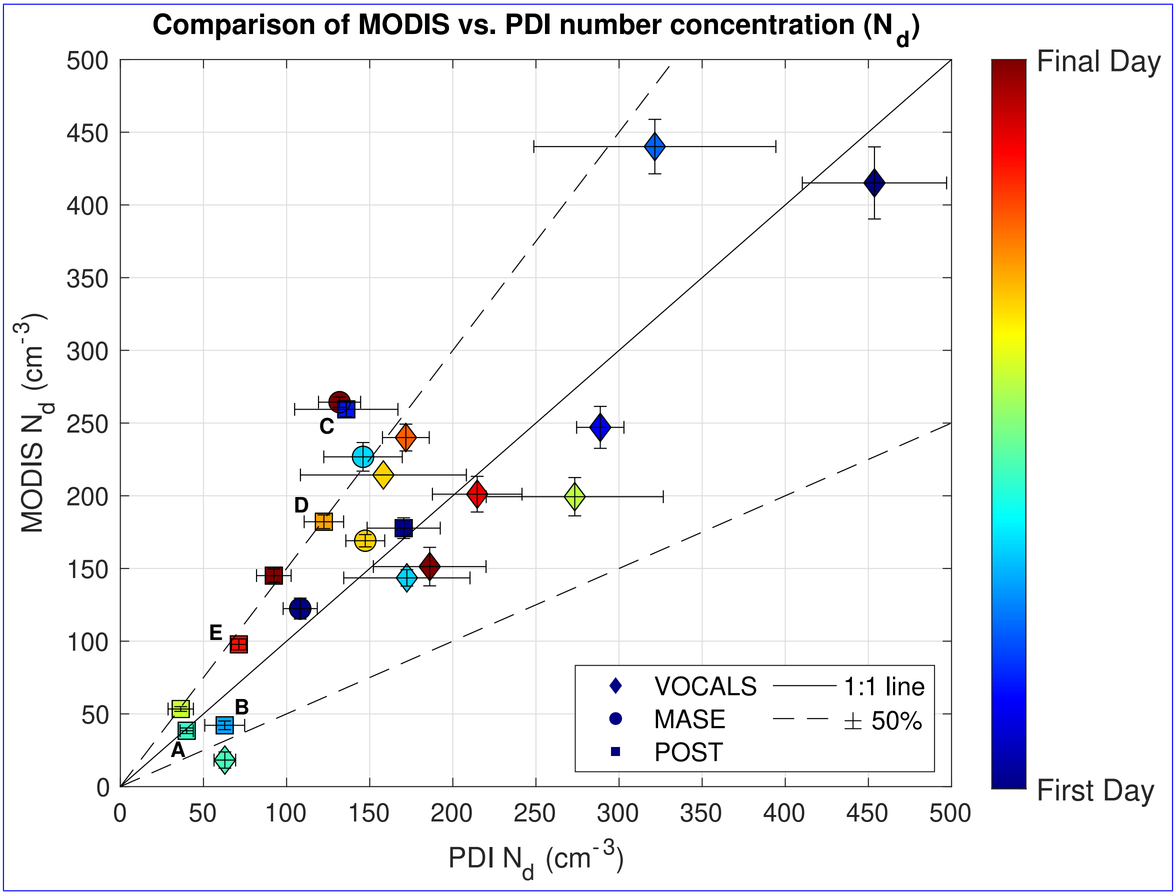

Figure 1. Comparison of MODIS number concentration vs PDI number concentration. PDI values are ~~N_d~~ N_{d} averaged at mid-cloud for all flight legs on that day, and the uncertainty bar represents 1σ variability of 1-km averaged values. Each flight campaign is marked by a symbol with color ranging from the first day of the campaign to the last. Several POST days are labeled A to E which represent specific cases discussed in Section 3.3. The MODIS ~~N_d~~ N_{d} value is a 1 km average of a 5×5 km^2 swath (with 1σ variability uncertainty bars) using Eq. 1 where effective radius and optical depth are taken from the satellite products. A linear fit of the data produces a slope of 1.1 ± 0.14.

a slope of 1.1 ± 0.14 (95% confidence interval). Although the one-to-one line is included in this confidence interval, there is a suggestion of an overestimation bias. However, because of the limited sample size it is unclear if this is statistically significant.

There are several questions which arise from this result. First, when MODIS and PDI number concentration are in very good agreement ~~,~~ (i.e., within sampling uncertainty of each other), is the satellite retrieved ~~N_d~~ N_{d} correct for the right underlying reasons or are there multiple errors which offset each other? Second, when MODIS disagrees with PDI, which MODIS retrieval products and/or assumptions are responsible for the discrepancy? To investigate these questions, we further analyze and compare the underlying variables in the MODIS ~~N_d~~ N_{d} retrieval.

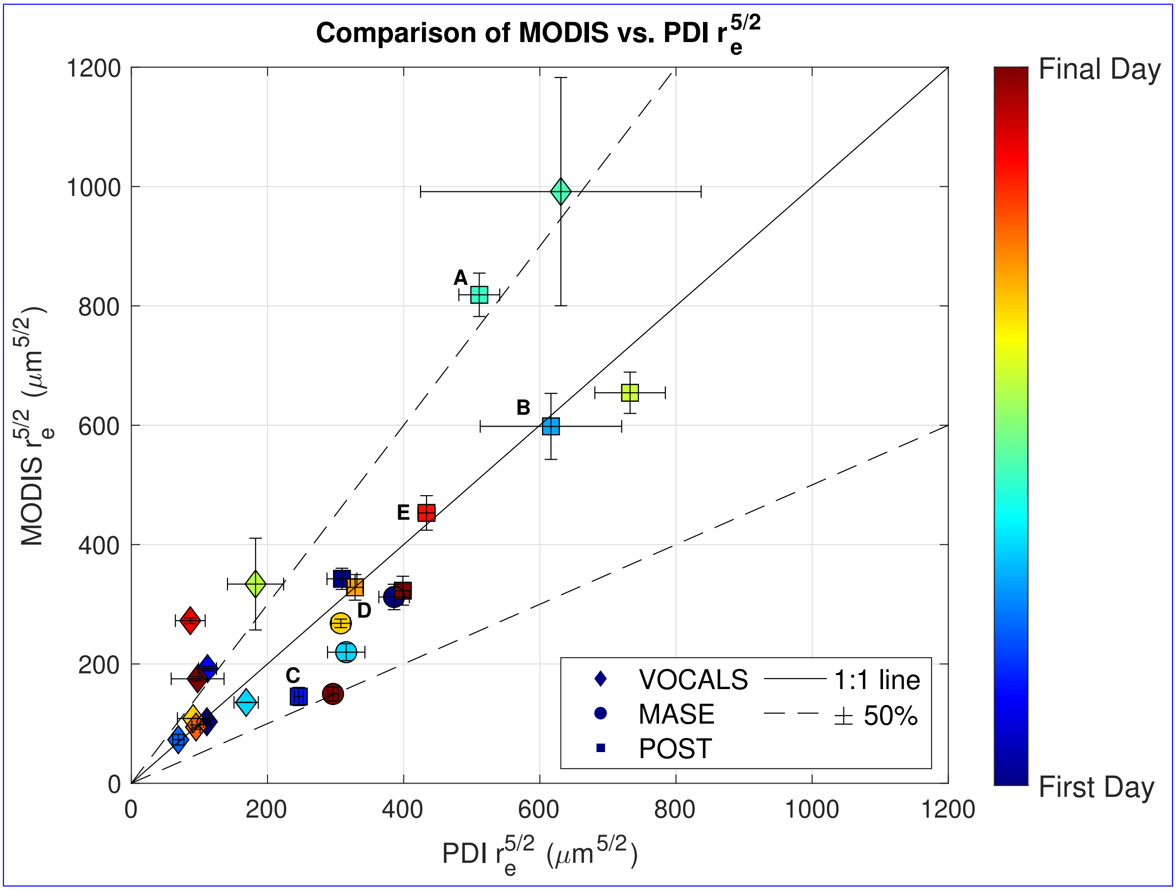

Figure 2. Comparison of $r_e^{5/2}$ between PDI measurements and the MODIS retrieved values. Satellite effective radius is ~~a~~ the average of 5×5 km^2 swaths of the MODIS ~~r_e~~ r_e product. The PDI value is ~~r_e~~ r_e averaged for all cloud top flight legs on that day. A linear fit of the data produces a slope of 1.0 ± 0.07. Labels and uncertainty bars are the same as in Fig. 1.

3.2 Comparison between MODIS and PDI $r_e^{5/2}$

Effective radius is the most influential term in the ~~N_d~~ N_d calculation, and thus ~~we~~ it's logical to speculate that good agreement between satellite and in situ ~~r_e values would likely~~ r_e values would manifest as good agreement between PDI and MODIS number concentration. Because MODIS ~~$N_d \propto r_e^{-5/2}$~~ $N_\mathrm{d} \propto r_\mathrm{e}^{-5/2}$ (Eq. 1), Fig. 2 compares MODIS and in situ $r_e^{5/2}$ values across the three campaigns.

Fig. 2 shows that there is a range of agreement between PDI and MODIS, with most of the days agreeing to within 25%. A linear regression of the data produces a slope of 1.0 ± 0.07 (95% confidence interval). This is a result consistent with Witte et al. (2018) who found no significant bias between MODIS and PDI measured ~~r_e~~ r_e. Additionally, if ~~r_e~~ r_e were the determining factor in the accuracy of MODIS ~~N_d~~ N_d retrievals, it would be expected that the potential high bias of MODIS ~~N_d~~ N_d (Fig. 1)

	Symbol	Campaign	Date	%Discrepancy ~~r_e~~ r_{e}	%Discrepancy ~~N_d~~ N_{d}
Good N_{d} Agreement					
Good r_{e} Agreement	■	POST	2008/07/16	-6.8%	$+4.1\%$
Poor ~~r_e~~ r_{e} Agreement	◆	VOCALS	2008/11/10	$+37.0\%$	$+4.0\%$
Poor N_{d} Agreement					
	Symbol	Campaign	Date	%Discrepancy ~~r_e~~ r_{e}	%Discrepancy ~~N_d~~ N_{d}
Good ~~r_e~~ r_{e} Agreement	■	POST	2008/08/04	-0.04%	$+33\%$
Poor ~~r_e~~ r_{e} Agreement	◆	VOCALS	2008/11/01	$+17\%$	-250%

Table 1. Examples of each of the four possible combinations of ~~N_d~~ N_{d} and ~~r_e~~ r_{e} agreement with their associated campaign, day, discrepancy, and corresponding symbol from Figs. 1 and 2. The finding that at least one case has a large discrepancy (37%) in effective radius, with a small discrepancy (4%) in ~~N_d~~ N_{d} implies that there are compensating errors in other retrieval parameters. In other words, it is possible to retrieve the right ~~N_d~~ N_{d} for the wrong underlying reasons.

would correspond to a low bias in MODIS ~~r_e~~ r_{e}. The data does not support this hypothesis, implying that the problem with the satellite estimation cannot solely be attributed to effective radius.

On an individual flight basis, comparing Fig. 2 and Fig. 1 shows that agreement in ~~N_d~~ N_{d} does not necessarily equate to agreement in $r_e^{5/2}$ and vice versa. In fact, there are four different scenarios which occur:

1. Agreement in $r_e^{5/2}$ with agreement in ~~N_d~~ N_{d}.
2. Agreement in $r_e^{5/2}$ with disagreement in ~~N_d~~ N_{d}.
3. Disagreement in $r_e^{5/2}$ with agreement in ~~N_d~~ N_{d}.
4. Disagreement in $r_e^{5/2}$ with disagreement in ~~N_d.~~ N_{d}.

We illustrate one example of each case in Table 1. The finding that the ~~r_e~~ r_{e} retrieval does not govern agreement of MODIS ~~N_d~~ N_{d} leads us to further investigate the other variables in the MODIS ~~N_d~~ N_{d} calculation.

3.3 Specific POST cases

The MODIS calculation for number concentration implicitly relies on vertical profiles of L ~~(through k and f_{ad}), r_e~~, r_{e}, and β~~(through τ_c)~~. These profiles combine MODIS measurements of ~~τ_c and r_e~~ τ_{c} and r_{e} with assumptions of cloud vertical structure (see Section 1.1). We compare these profiles with those measured by aircraft during the POST campaign. The sawtooth flight plan of POST allows for detailed profile comparisons. Five POST cases are selected to illustrate the range of behaviors observed across all eight POST flights analyzed in this manner. Fig. 3 illustrates the amount of data for four of the cases. Most of the data is concentrated within 150 m of cloud top. It is difficult to make statistically robust conclusions at altitudes below this region. Within these eight cases, we find ~~one~~ two with excellent agreement between all observed and retrieved properties (~~Case 1~~one of which is explored in depth, Case A). The other ~~seven~~ six are cases where ~~N_d~~ N_{d} is not accurately retrieved. Among

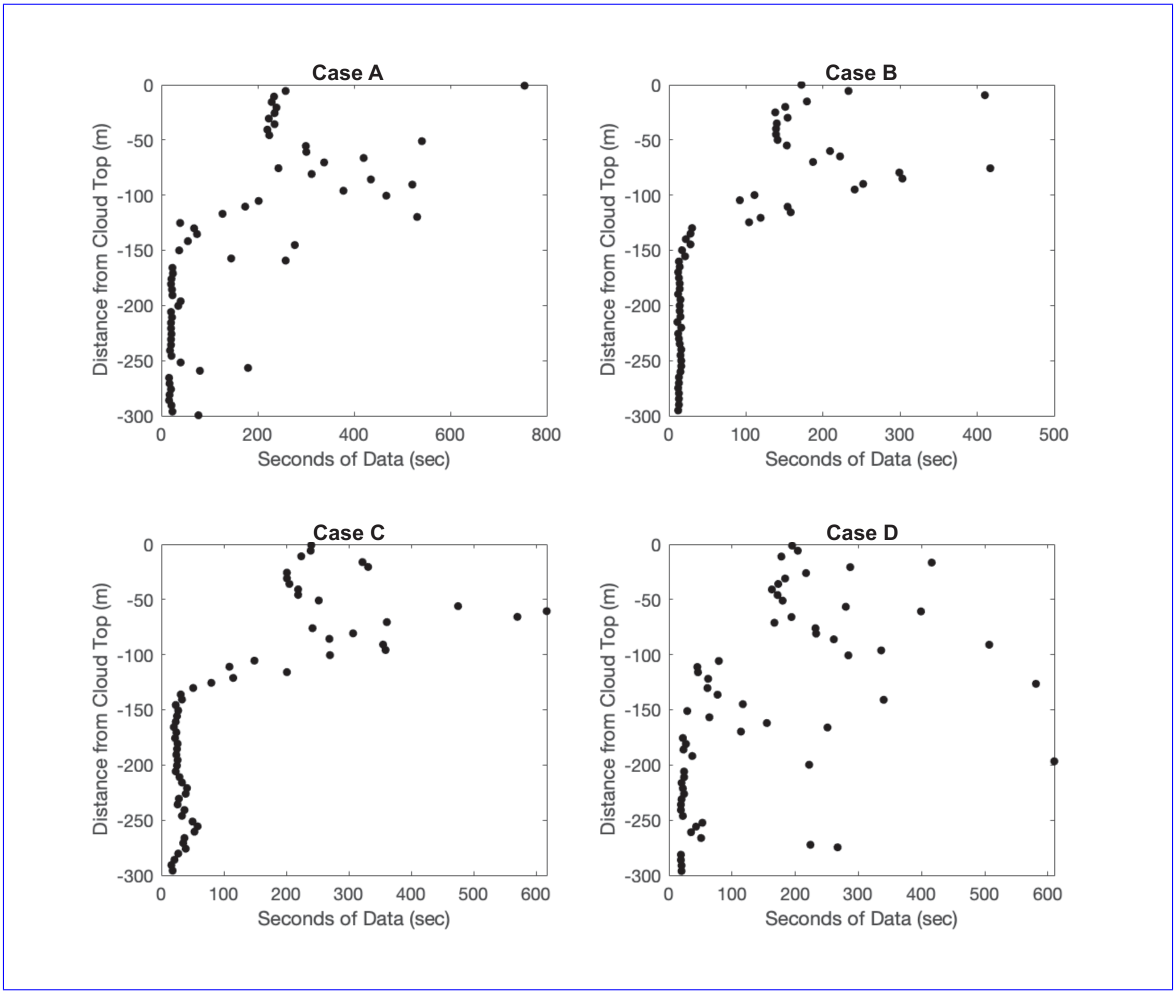

Figure 3. Amount of data for four of the five POST flights selected for additional analysis. Points represent seconds of non-zero data within each 5 m ~~z_{shift}~~ z_{shift} altitude bin and are concentrated within ∼150 m of cloud top.

these cases, none represents an accurate retrieval of ~~N_d~~ N_{d} with significant errors in the underlying retrieval properties that compensate for each other, although such cases do exist (see Table 1).

3.3.1 Case ~~1~~A: POST day 2008/07/30

Case A (Fig. 4) is an example of the best case scenario for agreement between MODIS and in situ profiles. The PDI observed number concentration (open circles) calculated at mid-cloud is ~~$N_d = 40 \pm 2$~~ $N_{\text{d}} = 40 \pm 2$ cm^{-3}, while MODIS estimates ~~$N_d = 38 \pm 4$~~ $N_{\text{d}} = 38 \pm 4$ cm^{-3} (solid red line). The satellite assumes that this number concentration is fixed throughout the vertical cloud profile. In reality ~~N_d~~ N_{d} is not constant with height, but instead gradually drops off towards cloud base and cloud top. We attribute lower values of ~~N_d~~ N_{d} near cloud top to cloud drop evaporation due to ~~entrainment~~turbulent entrainment of warm, dry air from above the boundary layer. Low values near cloud base may be an effect of uneven cloud base~~.~~, which affects the altitude range over which activation causes N_d to increase with height. In addition, cloud base is typically higher in those portions of the cloud layer that experience downdrafts due to lower adiabaticity (Zhou and Bretherton, 2019), which can affect N_d in the cloud base region. Through the middle of the cloud ~~N_d~~ N_d does appear reasonably constant on average. Because constant ~~N_d~~ N_d is consistent with the MODIS assumption, we use this as justification for the use of mid-cloud level legs for the MODIS-PDI ~~N_d~~ N_d comparison.

The vertical profiles of L, ~~r_e~~r_e, and β all agree very closely during this flight. The MODIS estimate of cloud top ~~r_e~~ r_e (blue star) is plotted at an altitude determined by the weighting function (Eq. 3) and is consistent with aircraft measurements. Lastly, cloud base altitude as estimated from MODIS and aircraft (red and black dashed lines, respectively) also agree well. The alignment between this full set of MODIS and aircraft observations results in an accurate estimate of ~~N_d~~ N_d as long as we interpret this value as a mid-cloud estimate. However, this day represents ~~the only flight where this best case scenario~~ only two of the flights where agreement across all quantities occurs.

3.3.2 Case ~~2~~B: POST day 2008/07/21

Unlike the strong agreement between MODIS and PDI seen in Case ~~1,~~ A, Case B (Fig. 5~~(POST day 2008/07/21~~) illustrates a day in which all of the profiles have very poor agreement. The MODIS retrieved number concentration is ~~$N_d = 42 \pm 12$~~$N_\mathrm{d} = 42 \pm 12$ cm^{-3} while the in situ value is ~~$N_d = 63 \pm 3$~~$N_\mathrm{d} = 63 \pm 3$ cm^{-3}. This disagreement occurs despite the fact that the satellite cloud top effective radius (blue star) is well-matched to the PDI estimate (13.0 ± 0.9 µm vs. 13.0 ± 0.5 µm), indicating that cloud top ~~r_e~~ r_e is not the source of the ~~N_d~~ N_d disagreement.

While the MODIS and PDI ~~r_e~~ r_e profiles agree at cloud top, at all other altitudes MODIS greatly underestimates effective radius. All else being equal, this should lead to an overestimation of ~~N_d~~N_d, which is not what we see. Instead, we attribute the MODIS ~~N_d~~ N_d underestimation to disagreement with the MODIS ~~τ_c retrieval. The MODIS $\beta(z)$ is determined by the MODIS retrieved τ_c while the MODIS $L(z)$ is heavily dependent on the MODIS retrieved τ_c (see Section 1.1). Consequently, any~~ τ_c retrieval. Any error in MODIS ~~τ_c~~ τ_c propagates to both the β and L profiles. Integration of the MODIS β profile results in a ~~τ_c~~ τ_c value smaller than observed, leading to an underestimation of ~~N_d ($N_d \propto \tau_c^{1/2}$~~N_d ($N_\mathrm{d} \propto \tau_\mathrm{c}^{1/2}$) as seen in Fig. 5, as well as a cloud base that is too high, which is equivalent to a cloud that is too thin.

3.3.3 Case ~~3~~C: POST day 2008/07/17

During POST flight 2008/17/07, the MODIS number concentration is ~~$N_d = 260 \pm 31$~~$N_\mathrm{d} = 260 \pm 31$ cm^{-3}, almost ~~a~~ twice the PDI value of ~~$N_d = 140 \pm 5$~~$N_\mathrm{d} = 140 \pm 5$ cm^{-3} (Fig. 6). In contrast to ~~the 2008/07/21 case~~Case B, we attribute the cause of this disagreement to MODIS retrieved cloud top ~~r_e~~r_e. The β and L profiles are in close agreement, presumably because MODIS and ~~PDI τ_c~~ PDI-derived τ_c are in agreement. However, both the PDI cloud top ~~r_e~~ r_e as well as the PDI ~~r_e~~ r_e vertical profile are greater than the MODIS estimates, leading to the large overestimation of ~~N_d~~N_d.

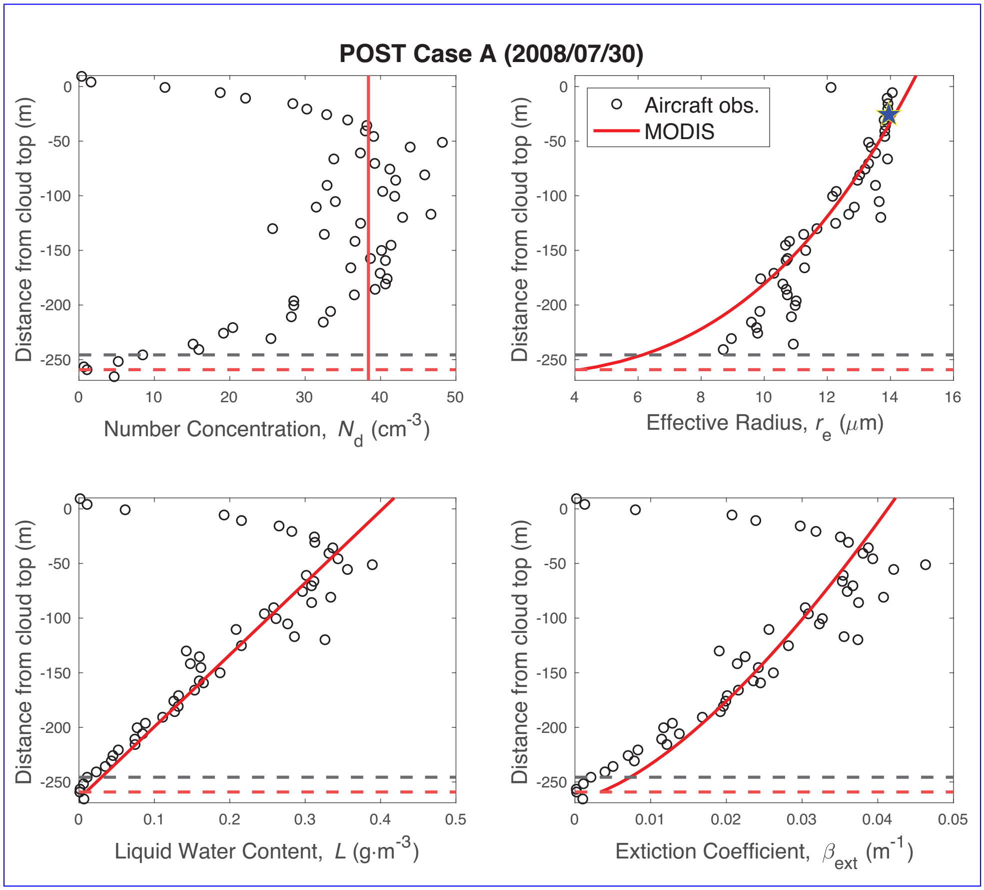

Figure 4. Profiles of ~~N_d, r_e~~ N_d, r_e, L, and β for POST ~~day~~ Case A (2008/07/30) comparing aircraft data (circles) and MODIS retrieval profiles (red lines). The aircraft measured cloud base is the black dashed line while the MODIS estimated cloud base is the red dashed line. Aircraft-derived ~~r_e~~ r_e that most closely corresponds to the MODIS cloud top value is indicated by the blue star, and is placed at an altitude determined by the max weight from Eq. 3. MODIS retrieval profiles of ~~N_d, r_e~~ N_d, r_e, L, and β are based on Eqs. 1, 10, 7, and 11, respectively.

3.3.4 Case ~~4~~D: POST day 2008/08/04

MODIS overestimates number concentration during POST ~~flight~~ Case D (2008/08/04), finding an ~~$N_d = 180 \pm 12$~~ $N_\mathrm{d} = 180 \pm 12$ cm^{-3} compared to a PDI value of ~~$N_d = 122 \pm 5$~~ $N_\mathrm{d} = 122 \pm 5$ cm^{-3} (Fig. 7). ~~More obviously, this~~ This case illustrates a day when the assumption that ~~N_d~~ N_d is constant with altitude is not accurate, with the retrieval overestimating ~~N_d~~ N_d at all altitudes. The ~~r_e~~ r_e subplot shows that there is good agreement between PDI and MODIS in both the cloud top ~~r_e~~ r_e value as well as the ~~r_e~~ r_e vertical profile (in the region of most influence, i.e. within 50 m of cloud top). However, the MODIS β and L profiles differ to a substantial degree from PDI. The MODIS β profile is greater than what is observed, meaning that the MODIS ~~τ_c~~ τ_c is also greater than the PDI value. Due to the relationship between ~~τ_c and N_d~~ τ_c and N_d, it follows that an overestimation in MODIS optical depth should lead to an overestimation in ~~N_d~~ N_d which is indeed what we see in Fig. 7.

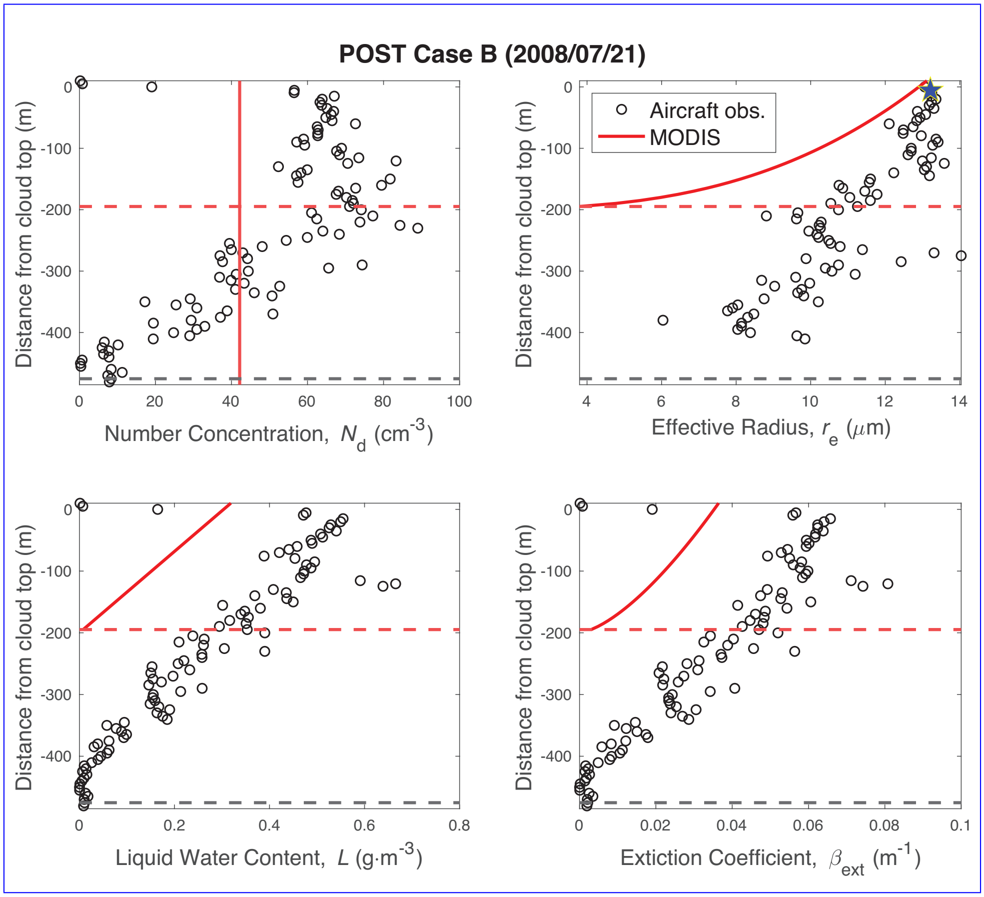

Figure 5. Comparison of profiles of ~~N_d, r_e~~ N_d, r_e, L, and β from aircraft observations (circles) and MODIS retrievals (red lines) for POST ~~on~~ Case B (2008/07/~~21.~~ 21). See Fig. 4 for more details.

3.3.5 Case ~~5~~E: POST day 2008/08/14

POST ~~flight~~ Case E (2008/08/14) illustrates the degree of sensitivity in the MODIS ~~N_d~~ N_d retrieval. Although the agreement between the profiles of ~~r_e~~ r_e, L, and β is not perfect, it is reasonably close (Fig. 8). Despite this, MODIS significantly overestimates number concentration (~~$N_d = 98 \pm 5$~~ $N_\mathrm{d} = 98 \pm 5$ cm^{-3} compared to the PDI value of ~~$N_d = 71 \pm 4$~~ $N_\mathrm{d} = 71 \pm 4$ cm^{-3}). Even small errors in effective radius manifest as a large error in number concentration, presumably due to the non-linear relationship between the two. This suggests that satellite profile estimates must be fairly accurate in order to successfully retrieve ~~N_d~~ N_d.

3.3.6 Summary of POST Cases

Based on POST profile analysis of the important variables that determine MODIS number concentration, we find that there are cases in which all variables agree well with PDI ~~observation~~ observations as well as cases where one or more variables disagree.

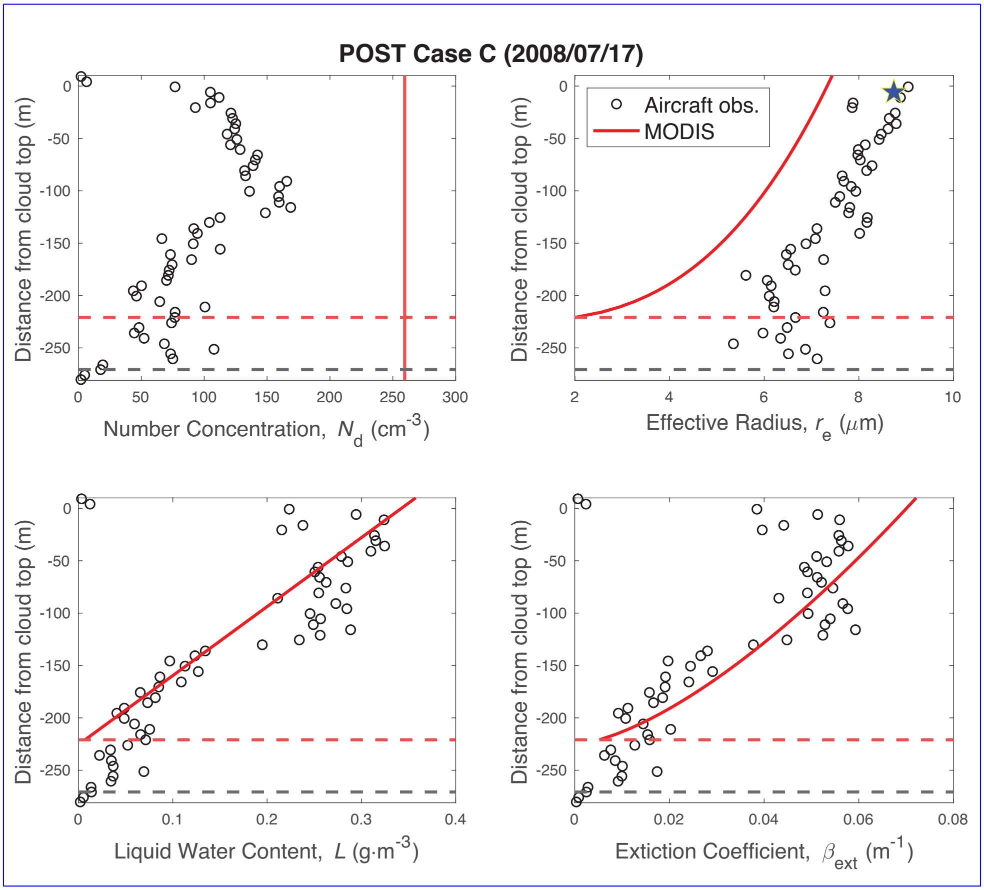

Figure 6. Comparison of profiles of ~~N_d, r_e~~ N_d, r_e, L, and β from aircraft observations (circles) and MODIS retrievals (red lines) for POST ~~on~~ Case C (2008/07/~~17.~~17). See Fig. 4 for more details.

However, out of all eight days considered, there are no cases in which the MODIS ~~N_d~~ N_d was correct due to compensating errors in the underlying variables (i.e. β, L, ~~r_e~~ r_e). If the satellite number concentration is a match to the in situ value, it is due to correct estimations in all variables. Conversely, if even one variable disagrees with observation, ~~N_d~~ N_d is also inaccurate. Fairly good agreement in all three profiles can also still yield significant discrepancy in ~~N_d.~~ N_d.

3.4 Analysis of k and ~~f_{ad}~~ f_ad

The accuracy of the MODIS assumptions concerning ~~f_{ad}~~ f_ad and k can also affect retrieved number concentration. The MODIS retrieval assumes that ~~f_{ad} is a constant equal to~~ f_ad has a constant value of 0.6. If ~~f_{ad}~~ f_ad were significantly different from this assumed value, we would find that the assumed MODIS slope of $L(z)$ would disagree with observations. We find that for each of the 8 POST flights, the in situ $L(z)$ slopes are well matched to MODIS, even if the absolute values are in disagreement. This leads us to conclude that ~~f_{ad}~~ f_ad has little effect on the ~~N_d~~ N_d retrieval for the cases that we analyzed.

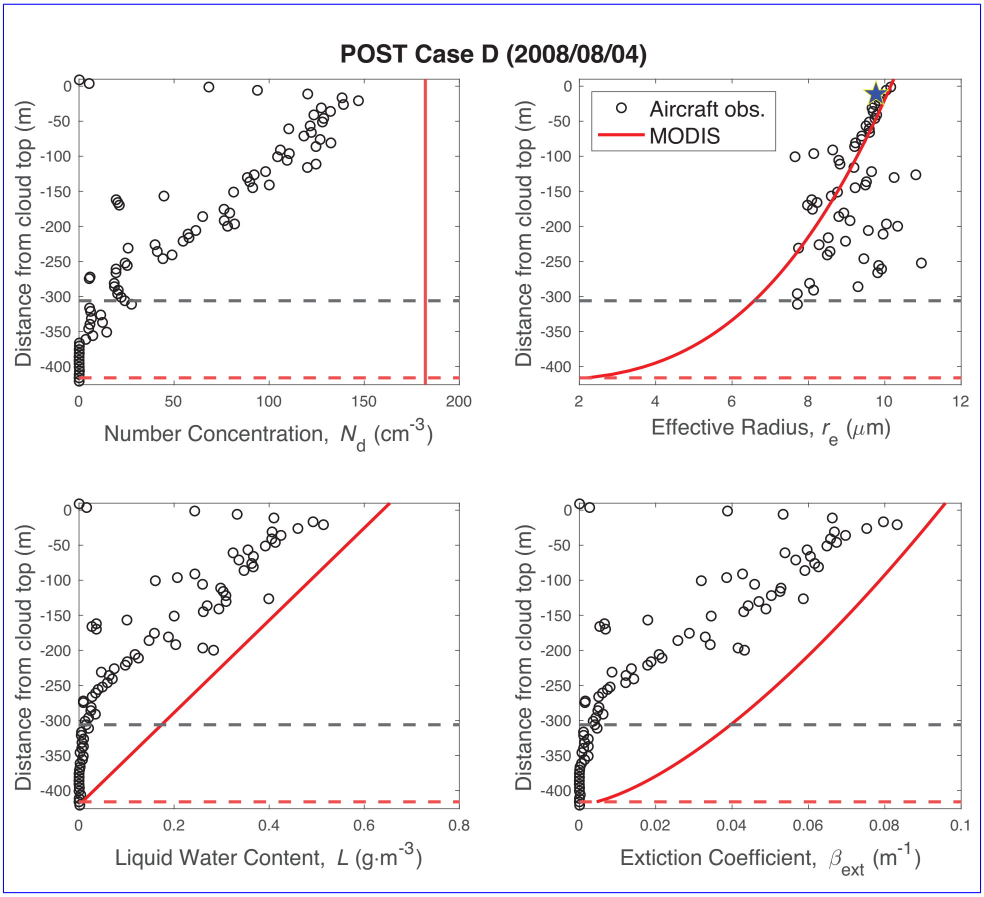

Figure 7. Comparison of profiles of ~~N_d~~ N_d, ~~r_e~~ r_e, L, and β from aircraft observations (circles) and MODIS retrievals (red lines) for POST ~~on~~ Case D (2008/08/~~04.~~ 04). See Fig. 4 for more details.

~~MODIS~~ The MODIS N_d retrieval assumes k is a constant of value 0.8. Analysis by Grosvenor et al. (2018) concludes that k ranges ~~$0.7 \le k \le 0.9$~~ from 0.7 to 0.9 (see also Lebsock and Witte, 2023). We evaluate this conclusion using the POST data (two examples shown in Fig. 9). Through the bulk of cloud profiles, the MODIS algorithm assumption is found to be generally reasonable. An uncertainty in k of ± 0.1 will lead to an uncertainty in N_d of 10 to 15%. Near cloud base, k can be much smaller. However, this can be considered inconsequential, as this region contributes little to the MODIS retrievals. There are also cases in which k exceeds this range near cloud top. However, occasional outlying behavior should not have a large impact on the retrieval and by default ~~N_d~~ N_d as well.

3.5 Determination of Cloud Base

As illustrated by Fig. 5, the large inaccuracies in the MODIS profile assumptions for POST ~~day 2008/07/21~~ Case B are accompanied by a large satellite overestimation of cloud base altitude (over 200 m difference from observed). Fig. 10 compares MODIS derived cloud base to the observed cloud base altitude for all eight of the POST flights. MODIS ~~is~~ estimates cloud

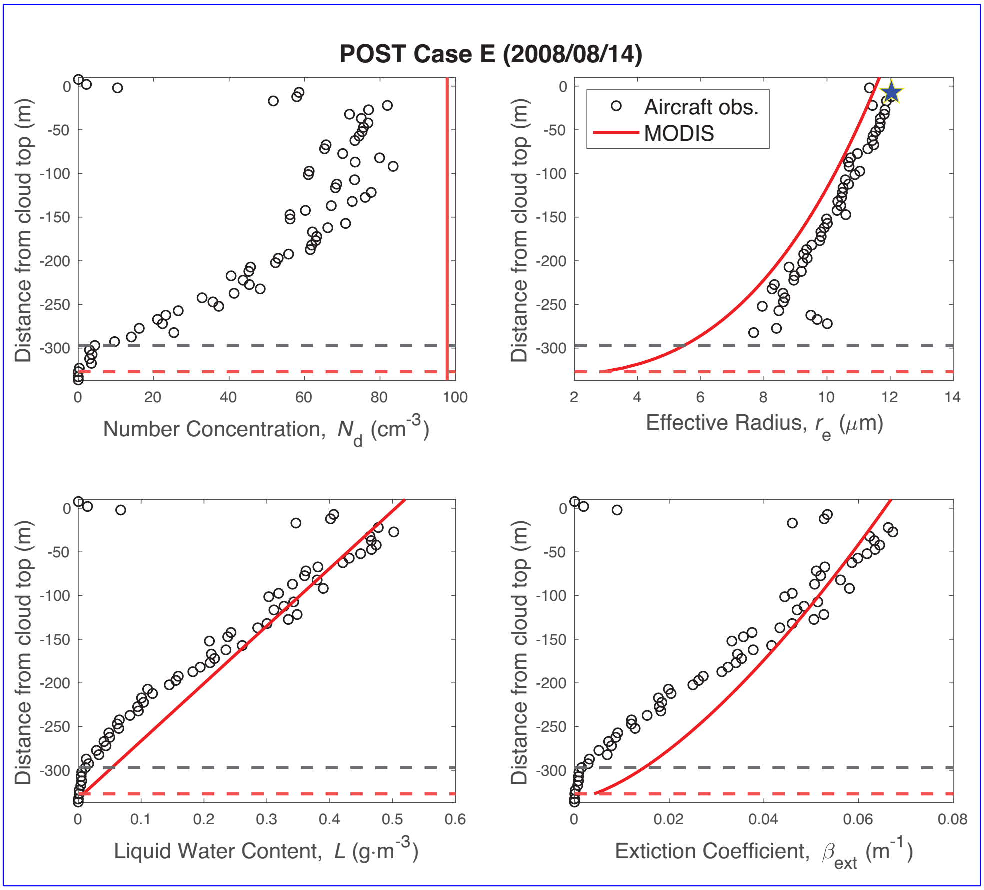

Figure 8. Comparison of profiles of ~~N_d, r_e~~ N_d, r_e, L, and β from aircraft observations (circles) and MODIS retrievals (red lines) for POST ~~on~~ Case E (2008/08/~~14.~~14). See Fig. 4 for more details.

base height within 50 m of ~~observation~~ the aircraft observations in 5 of the 8 cases. For the remaining three cases, MODIS cloud base differs by over 100 m, which is particularly notable since this is a significant fraction of the cloud depth. Due to the small sample size, however, it is difficult to quantify the frequency of accurate MODIS estimations of cloud base.

4 Conclusions

In this study, we compare ~~N_d~~ N_d derived from MODIS products with in situ observations recorded by the PDI instrument over three different field campaigns (MASE, VOCALS, and POST) sampling marine stratocumulus clouds. We also compare cloud microphysical and radiative variables relevant to the calculation of ~~N_d~~ N_d using observations from the POST campaign. These variables include vertical profiles of ~~r_e~~ r_e, L, and β.

Our results show that while there are instances in which ~~MODIS~~ the MODIS retrieval predicts number concentration within sampling variability, there are a significant number of cases in which the satellite overestimates ~~N_d~~ N_d. Our results suggest

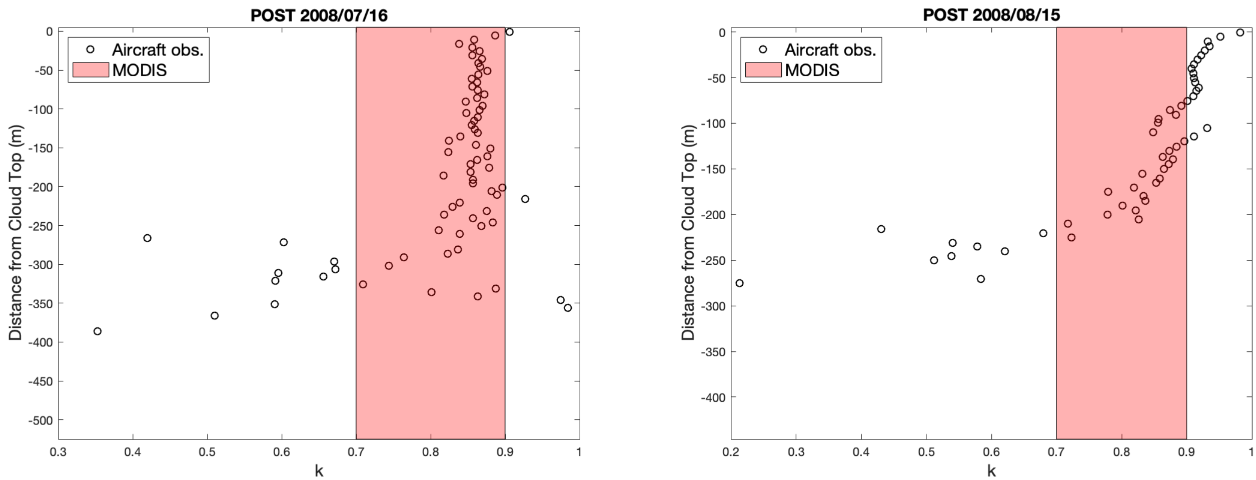

Figure 9. Comparison of k values from the POST campaign for days 2008/07/16 and 2008/08/15 with the MODIS assumed range of $0.7 \leq k \leq 0.9$ (red shading). The PDI values are calculated using Eq. 6 and represent flight averages at each 5 m z_{shift} z_{shift} bin.

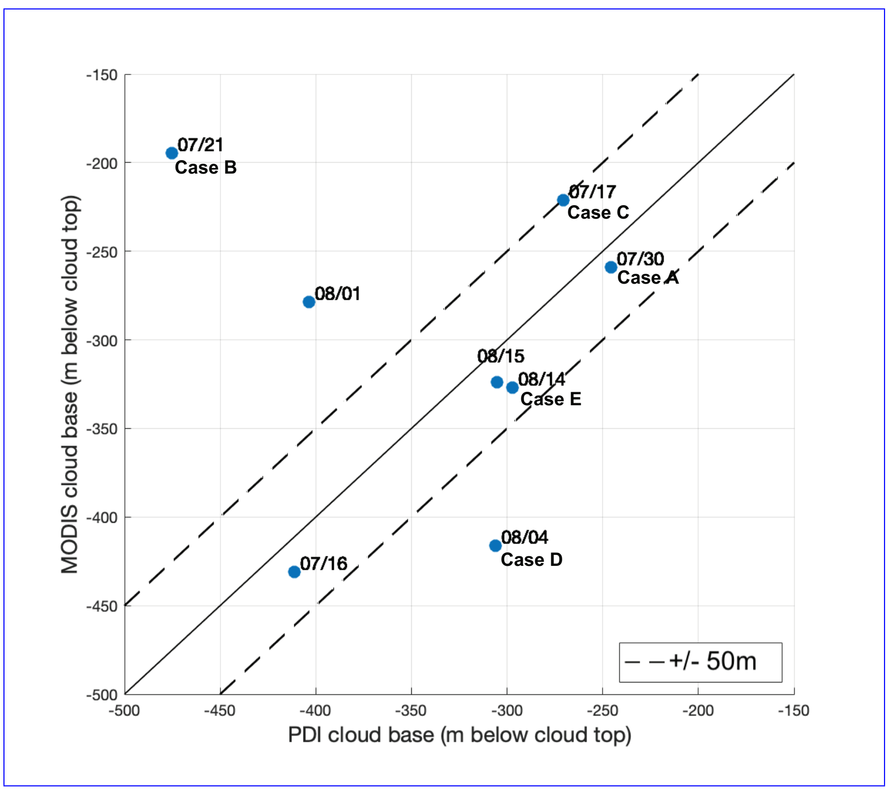

Figure 10. Comparison of MODIS and aircraft-estimated cloud base altitude for each day of the POST campaign. The 1:1 line (solid), and ± 50 m lines (dashed) are also shown.

that the discrepancy between retrieved and in situ N_d can be N_d can be greater than $\pm50\%$or more, which is substantially larger than the $\pm25\%$ that is proposed by Grosvenor et al. (2018), roughly in line with the $\pm80\%$ overall uncertainty previously proposed (Bennartz, 2007; Grosvenor et al., 2018). We find that the apparent overestimation bias in number concentration does not originate as a bias in MODIS r_e r_e. This is consistent with the conclusions of Witte et al. (2018) which who found no obvious bias between MODIS and PDI derived effective radius. We also find that it is possible for N_d N_d to be accurately retrieved with a poor retrieval of r_e r_e, presumably due to compensating errors in other retrieval parameters.

Based on analysis of vertical cloud profiles of r_eTwo out of the 8 POST cases studied exhibit good agreement in N_d, as well as in the profiles of r_e, L, and $\beta$from the POST campaign. For the remaining six cases, we do not attribute N_d N_d discrepancy to a single error source. Instead, we show that there are several different cases which result in incorrect number concentration:

1. MODIS incorrectly predicts profiles of r_e r_e, L, and β

2. MODIS incorrectly predicts profiles of L and β but accurately estimates r_e r_e (either the full r_e r_e profile or at the most influential altitude near cloud top)

3. MODIS incorrectly predicts profiles of r_e r_e but accurately estimates L and β profiles

Accurate N_d We also show a case where all profiles appear to exhibit reasonably good but imperfect agreement, but the resulting N_d does not agree well at all due to compounding errors.

Accurate N_d retrievals are representative of mid-cloud values. Although MODIS assumes number concentration is constant through a cloud's vertical profile, even in the best case scenarios it appears to be a poor reflection of cloud top and cloud base conditions. We also show one case where the assumption that N_d N_d is constant with altitude is not accurate.

In order to improve the MODIS N_d N_d retrieval, it would be beneficial to acquire more data collected in a manner similar to the POST campaign, i.e., with repeated sawtooth-like penetrations through cloud top. Multiple profiles near cloud top allow for deeper analysis of the underlying variables in the retrieval which can be used to more accurately quantify sources of error.

Data availability. PDI data from POST and VOCALS are freely available at https://data.eol. ucar.edu, and from MASE at https://doi.org/10.5281/zenodo.1035928. MODIS Level 2 retrievals are available from https://search.earthdata.nasa.gov.

Author contributions. SRP performed the data analysis and wrote the manuscript. MKW and PYC designed the study concept, obtained data, and edited the manuscript.

Competing interests. The authors declare no competing interests.

Acknowledgements. We thank the CIRPAS Twin Otter pilots, crew and instrument scientists for their efforts to collect the data used in this study. MKW acknowledges support from the Office of Naval Research Marine Meteorology program under funding documents N0001424WX00817 and N0001424WX02198.

References

Bellouin, N., Quaas, J., Gryspeerdt, E., Kinne, S., Stier, P., Watson-Parris, D., Boucher, O., Carslaw, K. S., Christensen, M., Daniau, A.-L., Dufresne, J.-L., Feingold, G., Fiedler, S., Forster, P., Gettelman, A., Haywood, J. M., Lohmann, U., Malavelle, F., Mauritsen, T., McCoy, D. T., Myhre, G., Mülmenstädt, J., Neubauer, D., Possner, A., Rugenstein, M., Sato, Y., Schulz, M., Schwartz, S. E., Sourdeval, O., Storelvmo, T., Toll, V., Winker, D., and Stevens, B.: Bounding Global Aerosol Radiative Forcing of Climate Change, Reviews of Geophysics, 58, e2019RG000 660, https://doi.org/https://doi.org/10.1029/2019RG000660, e2019RG000660 10.1029/2019RG000660, 2020.

Bennartz, R.: Global assessment of marine boundary layer cloud droplet number concentration from satellite, Journal of Geophysical Research: Atmospheres, 112, https://doi.org/https://doi.org/10.1029/2006JD007547, 2007.

Bennartz, R. and Rausch, J.: Global and regional estimates of warm cloud droplet number concentration based on 13 years of AQUA-MODIS observations, Atmos. Chem. Phys., 17, 9815–9836, https://doi.org/10.5194/acp-17-9815-2017, 2017.

Carman, J. K., Rossiter, D. L., Khelif, D., Jonsson, H. H., Faloona, I. C., and Chuang, P. Y.: Observational constraints on entrainment and the entrainment interface layer in stratocumulus, Atmos. Chem. Phys., 12, 11 135–11 152, https://doi.org/10.5194/acp-12-11135-2012, 2012.

Christensen, M. W., Gettelman, A., Cermak, J., Dagan, G., Diamond, M., Douglas, A., Feingold, G., Glassmeier, F., Goren, T., Grosvenor, D. P., Gryspeerdt, E., Kahn, R., Li, Z., Ma, P.-L., Malavelle, F., McCoy, I. L., McCoy, D. T., McFarquhar, G., Mülmenstädt, J., Pal, S., Possner, A., Povey, A., Quaas, J., Rosenfeld, D., Schmidt, A., Schrödner, R., Sorooshian, A., Stier, P., Toll, V., Watson-Parris, D., Wood, R., Yang, M., and Yuan, T.: Opportunistic experiments to constrain aerosol effective radiative forcing, Atmospheric Chemistry and Physics, 22, 641–674, https://doi.org/10.5194/acp-22-641-2022, 2022.

Chuang, P. Y., Saw, E. W., Small, J. D., Shaw, R. A., Sipperley, C. M., Payne, G. A., and Bachalo, W. D.: Airborne phase doppler interferometry for cloud microphysical measurements, Aerosol Sci. Tech., 42, 685–703, https://doi.org/10.1080/02786820802232956, 2008.

Gerber, H., Frick, G., Malinowski, S. P., Jonsson, H., Khelif, D., and Krueger, S. K.: Entrainment rates and microphysics in POST stratocumulus, J. Geophys. Res. Atmos., 118, 12,094–12,109, https://doi.org/https://doi.org/10.1002/jgrd.50878, 2013.

Gordon, H., Glassmeier, F., and T. McCoy, D.: An Overview of Aerosol-Cloud Interactions, chap. 2, pp. 13–45, American Geophysical Union (AGU), ISBN 9781119700357, https://doi.org/https://doi.org/10.1002/9781119700357.ch2, 2023.

Grosvenor, D. P., Sourdeval, O., Zuidema, P., Ackerman, A., Alexandrov, M. D., Bennartz, R., Boers, R., Cairns, B., Chiu, J. C., Christensen, M., Deneke, H., Diamond, M., Feingold, G., Fridlind, A., Hunerbein, A., Knist, C., Kollias, P., Marshak, A., McCoy, D., Merk, D., Painemal, D., Rausch, J., Rosenfeld, D., Russchenberg, H., Seifert, P., Sinclair, K., Stier, P., van Diedenhoven, B., Wendisch, M., Werner, F., Wood, R., Zhang, Z., and Quaas, J.: Remote sensing of droplet number concentration in warm clouds: A review of the current state of knowledge and perspectives, Rev. Geophys., 56, 409–453, https://doi.org/https://doi.org/10.1029/2017RG000593, 2018.

Gryspeerdt, E., McCoy, D. T., Crosbie, E., Moore, R. H., Nott, G. J., Painemal, D., Small-Griswold, J., Sorooshian, A., and Ziemba, L.: The impact of sampling strategy on the cloud droplet number concentration estimated from satellite data, Atmospheric Measurement Techniques, 15, 3875–3892, https://doi.org/10.5194/amt-15-3875-2022, 2022.

Leandro, M. D.: Phase-Doppler Interferometry: Characterization and Emerging Applications, https://www.proquest.com/dissertations-theses/phase-doppler-interferometry-characterization/docview/2864733359/se-2?accountid=12702, 2023.

Lebsock, M. D. and Witte, M.: Quantifying the dependence of drop spectrum width on cloud drop number concentration for cloud remote sensing, Atmos. Chem. Phys., 23, 14 293–14 305, https://doi.org/10.5194/acp-23-14293-2023, 2023.

Lu, M.-L., Conant, W. C., Jonsson, H. H., Varutbangkul, V., Flagan, R. C., and Seinfeld, J. H.: The Marine Stratus/Stratocumulus Experiment (MASE): Aerosol-cloud relationships in marine stratocumulus, J. Geophys. Res. Atmos., 112, https://doi.org/https://doi.org/10.1029/2006JD007985, 2007.

McCoy, D. T., Bender, F. A.-M., Grosvenor, D. P., Mohrmann, J. K., Hartmann, D. L., Wood, R., and Field, P. R.: Predicting decadal trends in cloud droplet number concentration using reanalysis and satellite data, Atmospheric Chemistry and Physics, 18, 2035–2047, https://doi.org/10.5194/acp-18-2035-2018, 2018.

McCoy, I. L., McCoy, D. T., Wood, R., Regayre, L., Watson-Parris, D., Grosvenor, D. P., Mulcahy, J. P., Hu, Y., Bender, F. A.-M., Field, P. R., Carslaw, K. S., and Gordon, H.: The hemispheric contrast in cloud microphysical properties constrains aerosol forcing, Proceedings of the National Academy of Sciences, 117, 18 998–19 006, https://doi.org/10.1073/pnas.1922502117, 2020.

Mechoso, C. R., Wood, R., Weller, R., Bretherton, C. S., Clarke, A. D., Coe, H., Fairall, C., Farrar, J. T., Feingold, G., Garreaud, R., Grados, C., McWilliams, J., Szoeke, S. P. d., Yuter, S. E., and Zuidema, P.: Ocean Cloud Atmosphere Land Interactions in the Southeastern Pacific: The VOCALS Program, Bull. Amer. Meteorol. Soc., 95, 357–375, https://doi.org/10.1175/BAMS-D-11-00246.1, 2014.

Miles, N. L., Verlinde, J., and Clothiaux, E. E.: Cloud droplet size distributions in low-level stratiform clouds, J. Atmos. Sci., 57, 295–311, https://doi.org/10.1175/1520-0469(2000), 2000.

Min, Q., Joseph, E., Lin, Y., Min, L., Yin, B., Daum, P. H., Kleinman, L. I., Wang, J., and Lee, Y. N.: Comparison of MODIS cloud microphysical properties with in-situ measurements over the Southeast Pacific, Atmos. Chem. Phys., 12, 11 261–11 273, https://doi.org/10.5194/acp-12-11261-2012, 2012.

Noble, S. R. and Hudson, J. G.: MODIS comparisons with northeastern Pacific in situ stratocumulus microphysics, J. Geophys. Res. Atmos., 120, 8332–8344, https://doi.org/https://doi.org/10.1002/2014JD022785, 2015.

Painemal, D. and Zuidema, P.: Assessment of MODIS cloud effective radius and optical thickness retrievals over the Southeast Pacific with VOCALS-REx in situ measurements, J. Geophys. Res. Atmos., 116, D24 206, https://doi.org/10.1029/2011JD016155, 2011.

Platnick, S.: Vertical photon transport in cloud remote sensing problems, J. Geophys. Res. Atmos., 105, 22 919–22 935, https://doi.org/10.1029/2000JD900333, 2000.

Quaas, J., Arola, A., Cairns, B., Christensen, M., Deneke, H., Ekman, A. M. L., Feingold, G., Fridlind, A., Gryspeerdt, E., Hasekamp, O., Li, Z., Lipponen, A., Ma, P.-L., Mülmenstädt, J., Nenes, A., Penner, J. E., Rosenfeld, D., Schrödner, R., Sinclair, K., Sourdeval, O., Stier, P., Tesche, M., van Diedenhoven, B., and Wendisch, M.: Constraining the Twomey effect from satellite observations: issues and perspectives, Atmospheric Chemistry and Physics, 20, 15 079–15 099, https://doi.org/10.5194/acp-20-15079-2020, 2020.

Sorooshian, A., Feingold, G., Lebsock, M. D., Jiang, H., and Stephens, G. L.: On the precipitation susceptibility of clouds to aerosol perturbations, Geophysical Research Letters, 36, https://doi.org/https://doi.org/10.1029/2009GL038993, 2009.

Twomey, S.: The Influence of Pollution on the Shortwave Albedo of Clouds, Journal of Atmospheric Sciences, 34, 1149 – 1152, https://doi.org/10.1175/1520-0469(1977)034<1149:TIOPOT>2.0.CO;2, 1977.

Witte, M. K., Yuan, T., Chuang, P. Y., Platnick, S., Meyer, K. G., Wind, G., and Jonsson, H. H.: MODIS retrievals of cloud effective radius in marine stratocumulus exhibit no significant bias, Geophys. Res. Lett., 45, 10,656–10,664, https://doi.org/https://doi.org/10.1029/2018GL079325, 2018.

Zheng, X., Albrecht, B., Jonsson, H. H., Khelif, D., Feingold, G., Minnis, P., Ayers, K., Chuang, P., Donaher, S., Rossiter, D., Ghate, V., Ruiz-Plancarte, J., and Sun-Mack, S.: Observations of the boundary layer, cloud, and aerosol variability in the southeast Pacific near-coastal marine stratocumulus during VOCALS-REx, Atmos. Chem. Phys., 11, 9943–9959, https://doi.org/10.5194/acp-11-9943-2011, 2011.

Zhou, X. and Bretherton, C. S.: Simulation of Mesoscale Cellular Convection in Marine Stratocumulus: 2. Nondrizzling Conditions, Journal of Advances in Modeling Earth Systems, 11, 3–18, https://doi.org/https://doi.org/10.1029/2018MS001448, 2019.